GENERATION OF LOW-FREQUENCY ELECTRIC FIELD FLUCTUATIONS IN THE MAGNETOSPHERE

G.S. Lakhina

*Indian Institute of Geomagnetism,
Colaba,
Mumbai — 400 005*

ABSTRACT

Observations from many spacecrafts have established the presence of low-frequency electric field fluctuations (LEF) in the regions of magnetospheric flow boundaries like magnetopause, plasma sheet boundary layer, polar cusp/cleft and the auroral region. It is shown that in the presence of cold background electrons, a low freqency electrostatic instability can be excited on the auroral field lines by the upward moving ion beams. For typical auroral plasma parameters the instability can generate LEF in the frequency range of 10^{-2} Hz to about 60 Hz. The low frequency waves propagate nearly transverse to the auroral field lines, and can amplitude ~ 10 mV/m to as high as 1 V/m.

On the other hand, ion beams observed in the plasma sheet boundary layer and in the polar cusp have sufficient velocity shears to drive ion cyclotron instabilities propagating nearly transverse to the magnetic field $\mathbf{B_0}$. In the plasma sheet boundary layer, LEF generated by the velocity shear instabilities have frequencies in the range from 0.4 Hz to 4 Hz with wavelengths ~ 30 km to 400 km. In the polar cusp, these velocity shear instabilities can excite braodband LEF with frequencies varing from 2 Hz to 35 Hz.

INTRODUCTION

Several spacecraft namely OGO 3, IMP 6, Hawkeye 1, S3-3, GEOS 1 and· 2, Viking etc. have observed the low-frequency electric field fluctuations (LEF) with frequencies ranging from essentially zero to a few kHz in different regions of the Earth's magnetosphere, e.g., magnetopause [1, 2], plasmasheet boundary layer [3, 4], polar cusp (5, 6], dayside auroral oval [7], auroral field lines at altitudes of 6000 - 12 000 km [8, 9, 10, 11], and ring current region [12, 13]. Generally, the noise at the lowest frequencies is prodominantly electromagnetic in nature, whereas the fluctuations at the higher frequencies are mostly electrostaic in nature [6, 12, 14, 15 - 18].

Various mechanism have been proposed to explain the generation of LEF observed in different regions of the magnetosphere. These mechanisms had been usually motivated by the correlation of the low-frequency noise with currents, density gradients, ion or electron beams, velocity shears etc. Huba et al. [19] discussed lower hybrid drift (LHD) instability to explain the broadband electrostatic noise, observed by Gurnett et al. [4], in the magnetotail region . Gary and Eastman [20] proposed LHD instability as a possible candidate for the generation of LEF at the magnetopause. Coroniti [21] and Lakhina [22] have shown that, in the ring current region, a quasi-electrostatic instability driven by the loss-cone distribution of protons can produce LEF. Bhatia and Lakhina [23] have suggested a drift loss cone instability in the ring current and plasma sheet region as a possible mechanism for the LEF observed beyond plasmapause. Grabbe and Eastman [24], Ashour- Abdalla and Okuda [25], Dusenbury and Lyons [26] and Omidi [27] have explained the generation of broad band elctrostatic noise by the ion beam instabilities in the plasma sheet boundary layer. On the other hand Lakhina [28] has suggested the ion velocity shear instabilities as a possible mechanism for the LEF in the plasma sheet boundary layer as well as in the cusp region. Temerin [8] suggested that apparent frequency range of LEF in the spacecraft reference frame is the result of Doppler shifted zero frequency turbulence. Ion-ion two-stream instabilities, where the free energy for the modes comes from the relative streaming between two ion species, have been invoked to explain the low-frequency electrostaic noise observed on the auroral field lines [29, 30, 31, 32]. Recently Lakhina [33] has shown that precipitaing electrons and upward-moving ion beams can excite LEF on the auroral field lines.

In addition to the above linear instability mechanisms, several nonlinear methods have been suggested for the generation of LEF in the magnetosphere. To cite a few, Bell and Ngo [34] explained the *spectral broadening* of the 13.1 kHz Omega transmitter signals in terms of the generation of sideband elctrostatic waves (*sim* 130 Hz) during the scattering of elctromagnetic waves from density irregularities. Shukla and Bujarbarua [35] suggested that the upper hybrid waves can excite ELF fluctuations at the plasmapause by a parametric instability process. Roy and Lakhina [36] have shown that the parametric instability of lower hybrid pump waves can generate low frequency modes either at zero frequency or at the ion cyclotron frequency on the auroral field lines.

In this review, we shall discuss only those generation mechanisms for the low-frequency electric field fluctuations which involve energetic ion distributions or beams. There are several observations indicating the presence of energetic proton and heavier ion distributions in various regions of the magnetosphere. These energetic protons have, generally, non-Maxwellian distributions which can drive several plasma instabilities. Particle data from Explorer 45, AMPTE/CCE, GEOS 1 and 2, and other spacecrafts clearly indicate the presence of hot nonthermal proton distributions in the ring current region [19, 37 - 39]. Energetic ion dis

tributions have been observed on the auroral field lines, in the cusp/cleft region and in the plasma sheet boundary layer [9, 40 - 45]. Low-frequency electric field fluctuations driven by energetic ion beams can attain quite large amplitudes and therefore can lead to significant scatterring, heating and acceleration of the ions and electrons.

COLD ION BEAM INSTABILITIES

We shall discuss the generation of low frequency electrostatic modes (i.e., $n = 0$ Bernstein modes) driven by cold ion (H^+) beams moving upwards along the auroral field lines. The presence of cold background electrons plays an important role in this generation mechanism. The generation mechanism discussed here is conplementary to the ion- ion beam instability mechanism. For simplicity we consider only a single ion (i.e. H^+) beam only.

Let us describe the plasma in the auroral acceleration region by a simple model consisting of only three species [33]:

(1) hot electrons in the kev energy range, which are precipitated from either the ring current or plasma sheet region, with temperature T_H and density N_H, (2) cold background electrons with temperature T_C and density N_C, (3) an ion beam (say H^+ or O^+ moving upward away from the earth along the auroral field lines with drift speed U_i, temperature T_i and density N_i. The geomagnetic field will be considered as uniform, and pointing upwards along z - direction, i.e., $\mathbf{B_0} = B_0 \hat{z}$. The distribution functions for the hot electrons and the cold electrons are taken as Maxwellian. The distribution function for the ion beam would be taken as drifted Maxwellian. The system is considered to be charge neutral in the equilibrium state, i.e. $N_i = N_C + N_H$.

We shall discuss the low frequency electrostatic waves (i.e. $n = 0$ Bernstein modes) under the following assumptions :

(i) The wave frequencies are such that the condition $|\omega - k_{\parallel} U_j|^2 << \Omega_j^2$ is satisfied for each species. Here ω is the wave frequency, $\Omega_j = (e_j B_0 / m_j c)$ is the gyrofrequency of the jth species, where $j = $ H for hot electrons, C for the cold background electrons, and i for the ions.

(ii) The waves propagate nearly transverse to magnetic field i.e., $k_{\parallel}^2 << k_{\perp}^2$ where $k_{\parallel}$ and $k_{\perp}$ are respectively the parallel and perpendicular component of the wave vector $\mathbf{k}$.

(iii) The condition $\mu_{nj} \equiv (\omega - k_{\parallel} U_j - n\Omega_j)/2^{1/2} k_{\parallel} V_{tj} >> 1$ is satisfied for all species for $n \geq 1$. Here $V_{tj} = (T_j/m_j)^{1/2}$ is the thermal speed of the jth species.

The dispersion relation for the low frequency electrostatic waves under the assumptions

(i) to (iii) is given by [30, 33, 46]:

$$1 + X_H + X_C + X_i = 0, \tag{1}$$

where

$$X_j = \frac{\omega_{pj}^2}{k^2 V_{tj}^2}[1 + \Gamma(\lambda_j)\mu_{0j}Z(\mu_{0j})], \tag{2}$$

where $\omega_{pj} = (4\pi N_j e^2/m_j)^{1/2}$ is the plasma frequency, and $\Gamma(\lambda_j) = I_0(\lambda_j)e^{-\lambda_j}$, where $I_0(\lambda_j)$ is the modified Bessel's function with the argument $\lambda_j = (k_\perp^2 V_{tj}^2/\Omega_j^2)$. To solve the dispersion relation we make an additional assumption, namely

(iv) We treat the background electrons and the ion beam as cold i.e.,$\mu_{0i}^2 \gg 1$ and $\mu_{0c}^2 \gg 1$, and the precipitating electrons as hot i.e., $\mu_{0H} \leq 1$.

We shall discuss the fluid (nonresonant) instabilities driven by the ion beam.   Let $\omega = \omega_r + i\gamma$, where ω_r and γ represent respectively the real frequency and the growth rate. For the case of fluid instabilities $\gamma \sim \omega_r$ holds generally. On taking the limit of $\mu_{0C}^2 \gg 1$, $\mu_{0i}^2 \gg 1$ and $\mu_{0H}^2 \ll 1$ in Eq. (2), we get

$$X_C = \frac{\omega_{pC}^2}{\Omega_e^2} - \frac{k_\parallel^2 \omega_{pC}^2}{k^2 \omega^2}, \tag{3}$$

$$X_i = \frac{f\omega_{pi}^2}{\Omega_i^2} - \frac{k_\parallel^2 \omega_{pi}^2 \Gamma(\lambda_i)}{k^2(\omega - k_\parallel U_i)^2}, \tag{4}$$

$$X_H = \frac{\omega_{pH}^2}{k^2 V_{tH}^2}, \tag{5}$$

where $f = [1 - \Gamma(\lambda_i)]/\lambda_i$. Then, the dispersion relation (1) can be written in the form,

$$D(\omega, k) \equiv \Delta - \frac{k_\parallel^2 \omega_{pC}^2}{k^2 \omega^2} - \frac{k_\parallel^2 \omega_{pi}^2 \Gamma(\lambda_i)}{k^2(\omega - k_\parallel U_i)^2} = 0, \tag{6}$$

where

$$\Delta = 1 + \frac{\omega_{pC}^2}{\Omega_e^2} + \frac{f\omega_{pi}^2}{\Omega_i^2} + \frac{\omega_{pH}^2}{k^2 V_{tH}^2}. \tag{7}$$

We can rewrite Eq.(6) as

$$(\omega^2 - \omega_C^2)[(\omega - k_\parallel U_i)^2 - \omega_i^2] = \omega_C^2 \omega_i^2, \tag{8}$$

where

$$\omega_j = \pm \frac{k_\parallel \omega_{pi} \Gamma(\lambda_j)^{1/2}}{k \Delta^{1/2}}, j = C, i. \tag{9}$$
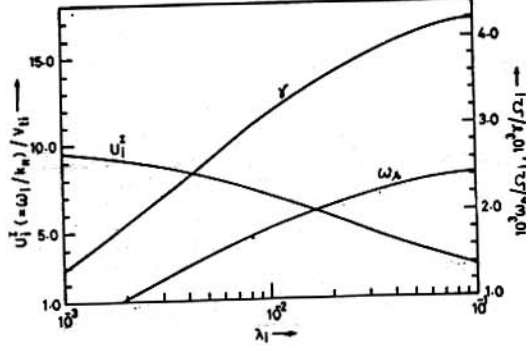
A. Mode 1 ion beam instability

69

Fig. 1 : Variation of ω_r/Ω_i , γ/Ω_i and U_i^I versus λ_i for the mode 1 ion beam instability for the auroral plasmas with $N_C = 0.001$ cm^{-3}, $N_H = 1$ cm^{-3}, $B_0 = 0.046$ G, $T_H = 1$ keV, $T_i = 10$ eV, $T_C = 0.01$ eV and $k_\parallel/k = 10m_e/m_i$. The assumption $\mu_{0i}^2 \gg 1$ tends to breakdown as $\lambda_i \to 0.1$ (after Lakhina [33]).

For $U_i \approx U_i^I = (\omega_i/k_\parallel)$, we get from (8) an unstable root

$$\omega = \left(\frac{\omega_C^2 \omega_i}{2}\right)^{1/3} \frac{(1 + i\,3^{1/2})}{2}, \tag{10}$$

provided $(\omega_{pC}^2/\omega_{pi}^2) < 2$.

In Figure 1, we have shown the variations of real frequency ω_r, growth rate γ, and the optimum velocity U_i^I against λ_i for the mode 1 ion beam instability relevant to auroral plasma parameters. As $\lambda_i \to 0.1$, the assumption of $\mu_{0i}^2 \gg 1$ breaks down and one has to treat ions as hot.

B. Mode 2 ion beam instability

On the hand, for $\omega \simeq k_\parallel U_i = k_\parallel U_i^{II} + \eta$, where $U_i^{II} = \omega_C/k_\parallel$ and $\eta \ll \omega_C$, (8) can be solved for η to get an unstable root with the growth rate

$$\gamma = I_m \eta = \frac{3^{1/2}}{2} \left(\frac{\omega_C \omega_i^2}{2}\right)^{1/3}, \tag{11}$$
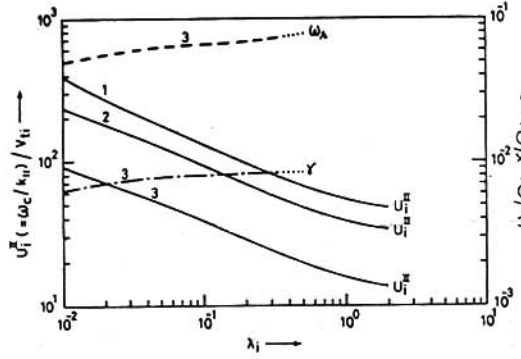
provided $(\omega_{pC}^2 \omega_{pi}^2) > 2$.

Fig. 2 : Variation of ω_r/Ω_i , γ/Ω_i and U_i^{II} versus λ_i for the mode 2 ion beam instability for $N_C = 10.0$, 1.0 and 0.1 cm^{-3} for the curves 1, 2 and 3 respectively. The rest of the parameters are the same as in Figure 1 except that $T_C = 0.1$ eV. The assumption of $\mu_{0i}^2 \gg 1$ tends to breakdown for $\lambda_i > 0.3$ (cf. dotted portion of ω_r and γ curves) (*after Lakhina [33]*).

Variations of ω_r, γ and U_i^{II} with λ_i for the mode 2 ion beam instability are shown in Figure 2. In this case the assumption of $\mu_{0i}^2 \gg 1$ breaks down for $\lambda_i \geq 0.3$.

Application to Auroral Region

In the auroral acceleration region between 1 to 2 R_E altitudes,we can take $\Omega_i = 70$ - 140 Hz. The density and energy of precipitating electrons are variable but in the general range of $N_H \sim (0.1$ - 1) cm^{-3}, and their energy $E_H \sim (0.1$ to 5) keV. We take typical value of hot electron temperature as $T_H = 1$ keV. This gives $V_{tH} = 1.32 \times 10^4$ km s^{-1}. Outside the region of strong parallel potential drops, the typical values of the background cold electrons parameters are $N_C \sim 10$ cm^{-3} or so, and $T_C = 1$ ev or less. But in the region of strong parallel electric fields the cold electrons are expelled resulting in $N_C = 10^{-3}$ cm^{-3} or smaller. The initial ion beam drift speed can be $U_i = (5$ - 50) V_{ti} and $V_{ti} = (9.8$ - 30.9) km s^{-1} corresponding to $T_i = 1$ to 10 eV. The density of ion beam could be calculated from the quasi- neutrality condition in the equilibrium state.

The results shown in Figure 1-2 are calculated for the plasma parameters corresponding to the auroral acceleration region described above. Further, the assumptions (i) to (iv) are

easily satisfied in the parametric range of $m_e/m_i < k_\parallel/k < (m_e/m_i)^{1/2}$, and $10^{-3} < \lambda_i < 1$. In these Figures we have fixed $k_\parallel/k = 10\ m_e/m_i$.

The ion beam driven mode 1, as seen from Figure 1, could be excited for beam drift speed $U_I \simeq U_i^I = (3\text{ - }10)\ V_{ti} \approx (90\text{ - }300)$ km s^{-1} for $10^{-3} < \lambda_i < 0.1$. The corresponding range of real frequencies ω_r, and growth rates γ are respectively, $\omega_r = (0.07\text{ - }0.16)$ Hz and $\gamma = (0.09\text{ - }0.29)$ Hz. The unstable perpendicular wavelengths $\lambda_\perp = 2\pi/k_\perp = 2\pi \rho_i/\lambda_i^{1/2}$, where $\rho_i = (V_{ti}/\Omega_i)$ is ion gyroradius, lie in the range of $1.4 km < \lambda_\perp < 14$ km for $\rho_i = 70$ m. The excitation of mode 2 driven by ion beam requires rather large beam drift speed $U_i \simeq U_i^{II} = (20\text{ - }400)V_{ti}$ unless $N_C < 0.1$ cm^{-3} (cf. Figure 2). For the case of $N_C = 0.1$ cm^{-3} and $U_i = (20\text{ - }50)V_{ti} \approx (600\text{ - }1500)$ km s^{-1}, as seen from Figure 2, this mode has $\omega_r \simeq (4.0\text{ - }5.0)$ Hz and $\gamma \simeq = (0.5\text{ - }0.6)$ Hz and unstable perpendicular wavelength $\lambda_\perp = (0.8\text{ - }2.0)$ km.

The parallel wavelength of these modes would be in the range of
$(m_i/m_e)^{1/2}\lambda_\perp < \lambda_\parallel < (m_i/m_e)\lambda_\perp$.

The low-frequency modes have a broadband spectrum and could be easily excited either by ion beams having drift speed 100 to 1500 km s^{-1} along the auroral field lines. In the references frame of a satellite moving with velocity of 7 km s^{-1}, the Doppler shifted frequencies of these modes would lie in the range between 10^{-2} Hz to 60 Hz. Hence the mechanism proposed here predicts the frequencies and wavelength in fairly good agreement with the observations from Viking [9] and from S3-3 [8].

Linear theory, like the one presented above, cannot provide any estimate for the saturation level of electric field fluctuations. However, estimates for the electric field fluctuations can be obtained by carrying out the quasilinear calculations [33]

It is found that mode 1 ion beam instability saturates at

$$E(t = \infty) \simeq \left[\frac{8\pi m_i N_i U_i \Omega_i^3 \Gamma(\lambda_i)^{1/2}}{\{1 + \frac{N_H \Gamma(\lambda_H)}{N_C} + \frac{m_e N_i \Gamma(\lambda_i)^2 \Omega_i^2}{k^2 U_i^2 f}\}\omega_{pi}^{4/3}\omega_{pC}^{2/3} f^{3/2} k} \right]^{1/2} \tag{12}$$

where as the mode 2 ion beam instability saturates at

$$E(t = \infty) \simeq \left[\frac{8\pi m_i N_i U_i \Omega_i^3 \omega_{pC}}{\{1 + \frac{N_H \Gamma(\lambda_H)}{N_C} + \frac{\Gamma(\lambda_i)\Omega_i^2}{k^2 U_i^2 f}\}\omega_{pi}^3 f^{3/2} k} \right]^{1/2}, \tag{13}$$

For $N_C = 10^{-3}$ cm^{-3}, $N_H = 1$ cm^{-3}, $B_0 = 0.046$ G, $T_i = 10$ ev, and $U_i = 5V_{ti}$ (corresponding to Figure 1), we get from Eq.(27), $E(t = \infty) = 60$ mV/m for mode 1.

Similarly, for $N_C = 0.1$ cm^{-3}, $N_H = 1$ cm^{-3}, $B_0 = 0.046$ G, $T_i = 10$ ev (i.e. corresponding to Figure 2) and $U_i = 40\ V_{ti}$, we get from Eq.(28), $E(t = \infty) \simeq 1$ V/m. We must keep in mind that the estimates for $E(t = \infty)$ for the ion beam instabilities given by Eqs.(27) -(28) are the upper bounds on the amplitudes.

The low-frequency electrostatic modes discussed here have several properties, like their broadband nature, their polarization and propagation direction, similar to those of the ion-ion two-stream modes [32] and the lower hybrid modes [36, 47 - 48]. However, the low-frequency electric-field fluctuations can heat the ions and the electrons only in the direction parallel to the magnetic field. Therefore, these modes could not lead to the formation of ion conics, but can form accelerated electron and hot ion beams. The analysis must be extended to include $n \geq 1$ modes to produce transverse heating of the ions leading to the formation of ion conics. The modes driven by ion beams would result in accelerated electron beams moving upwards in the direction of the ion beams. The above mechanism would work independent of the presence of a d.c. parallel electric field in the region of interaction.

HOT ION BEAM VELOCITY SHEAR INSTABILITY

The plasma sheet boundary layer and the cusp region are characterized by the plasma consisting of three components, namely, (1) background cold Maxwellian ions with number density, N_{0i}, and temperature, T_i, (2) warm background electrons characterized by Maxwellian distribution with number density, N_{0e}, and temperature, T_e, and (3) a low density hot ion beam streaming along the magnetic field $\mathbf{B}_0 = B_0(x)\mathbf{z}$ with a sheared velocity $\mathbf{V}_B = V_B(x)\mathbf{z}$ and having a number density, N_{0B}, and temperature, T_B. We consider $N_{0e} = N_{0i} + N_{0B}$ so that the charge neutrality is maintained in the equilibrium state. For simplicity, we shall neglect the density gradients of the background plasma and that of the ion beam. Furthermore, we shall not discuss the Kelvin-Helmholtz type instabilities here as these instabilitites have been discussed extensively in the literature [28, 49 - 53]. We shall concentrate on the cyclotron instabilities driven by the hot ion beam [28]. Therefore, we consider the frequency range $\omega \simeq n\Omega_B \ll \Omega_e$. For warm electrons, $\omega/k_{\parallel}V_{te} < 1$, and we can write

$$X_e \simeq \frac{\omega_{pe}^2}{k^2 V_{te}^2} + \frac{i\sqrt{\pi}\omega\omega_{pe}^2}{\sqrt{2}k_{\parallel}k^2 V_{te}^3} \exp\left[-\frac{\omega^2}{2k_{\parallel}^2 V_{te}^2}\right] \qquad (14)$$

The cold ion response can be written as

$$X_i = -\frac{\omega_{pi}^2 k_{\perp}^2}{(\omega^2 - \Omega_i^2)k^2} - \frac{k_{\parallel}^2 \omega_{pi}^2}{k^2 \omega^2}, \qquad (15)$$

Since a low density hot ion beam can not significantly affect the real frequency for the resonant type instability, the real frequency is given by $(1 + X_i + \Re X_e) = 0$, where $\Re X_e$ is

the real part of X_e. For $(\Omega_i^2 + k^2 C_s^2)^2 \gg 4k_\parallel^2 C_s^2 \Omega_i^2$, this leads to the following roots:

$$\omega_r^2 \simeq \Omega_i^2 + \frac{k^2 C_s^2}{1 + k^2 \lambda_{De}^2}, \tag{16}$$

and

$$\omega_r^2 \simeq \frac{k_\parallel^2 C_s^2 \Omega_i^2}{\Omega_i^2(1 + k^2 \lambda_{De}^2) + k^2 C_s^2} \tag{17}$$

The above roots describes the fast ion acoustic mode and the slow ion acoustic mode respectively. Here we are concerned with the fast ion acoustic mode only.

The hot ion beam introduces an imaginary term $\Im X_B$ in the dispersion relation given by

$$\Im X_B \simeq \frac{i\sqrt{\pi}\omega_{pB}^2}{\sqrt{2}k_\parallel k^2 V_{tB}^3} \sum_n \Gamma_n(\lambda_B)[(\omega_r - k_\parallel V_B) - \frac{k_\perp}{k_\parallel}S(\omega_r - k_\parallel V_B - n\Omega_B)]\exp(-\mu_{nB}^2), \tag{18}$$

where $S = \frac{1}{\Omega_B}\frac{dV_B}{dx}$ reperesents the velocity shear of the ion beam, $\mu_{nB} = (\omega - k_\parallel V_B - n\Omega_B)/2^{1/2}k_\parallel V_{tB}$, and $\Gamma_n(\lambda_B) = I_n(\lambda_B)e^{-\lambda_B}$.

Since ω_r of the fast ion acoustic mode changes with k, we can anticipate a situation where $\mu_{mB} \sim 1$ but $\mu_{nB} \gg 1$ for $n \neq m$. In such a case, only the $n = m$ term in $\Im X_B$ would be important. Then, the growth rate is given by

$$\gamma = \sqrt{\pi}\omega_r P \left[\frac{N_{0B}}{N_{0i}} \Gamma_m(\lambda_B) \left(\frac{Sk_\perp \mu_{mB}}{k_\parallel} - \mu_{0B} \right) \exp(-\mu_{mM}^2) - \frac{\omega_r}{\sqrt{2}k_\parallel V_{te}} \frac{T_B}{T_e} \exp\left(-\frac{\omega_r^2}{2k_\parallel^2 V_{te}^2} \right) \right], \tag{19}$$

where

$$P = \frac{\frac{\omega_r^2}{\Omega_i^2} \frac{k_\perp^2}{k_\parallel^2} \frac{m_B}{2m_i \lambda_B}}{1 + \frac{k_\perp^2}{k_\parallel^2} \frac{\omega_r^4}{(\omega_r^2 - \Omega_i^2)^2}} \tag{20}$$

It is interesting to note that for $\mu_{0B} > 0$, i.e., $\omega_r > k_\parallel V_B$ the instability is possible for for finite velocity shear, S, only. For a given m, the cyclotron instability can occur for as set of λ_B values at certain values of $k_\parallel/k$ as shown in Tables 1 and 2. By choosing a proper set of parameters like $k_\parallel/k$, λ_B, V_B/V_{tB}, and S, it is possible to excite the instability for harmonic number $m = 10$ or more.

Figure 3 shows the growth rate of the cyclotron instability for $m = 10$. The maximum in the growth rate is reduced and gets shifted towards higher λ_B by an increase in $k_\parallel/k$ (cf. curves 1, 2, 3 and 4). The growth rate is reduced when S decreases (cf. curves 1 and 5). From Tables 1 and 2, and Figure 3, we note that the unstable frequencies fall in the range $m\Omega_B < \omega_r < (m+1)\Omega_B$, and a broadband spectrum of waves, where various frequencies are propagating with slightly different oblique angles to $\mathbf{B}_0$, are generated by the cyclotron instability.

Table 1. Ion cycloton velocity shear instability for the case of $\omega_{pe}/\Omega_e=10.0$, $N_{0B}/N_{0i}=0.1$, $T_i/T_B=0.5$, $T_e/T_B=5.0$, $m_i/m_b=1.0$, $V_B/\sqrt{2}V_{tB}=10.0$, and $S=2.0$

$k_\parallel/k$	λ_B	m	ω_r/Ω_B	γ/Ω_B	μ_{0i}	μ_{0e}	μ_{mB}
0.058	0.45	1	1.58	-0.161	40.6	0.30	0.55
	0.50	1	1.63	0.121	39.6	0.29	0.91
	0.55	1	1.68	0.133	38.9	0.29	1.22
	0.9	1	1.73	0.032	38.3	0.28	1.51
	0.7	1	1.82	37.4	37.4	0.28	2.02
0.04	2.0	2	2.77	-0.321	48.8	0.36	-0.38
	2.3	2	2.95	0.270	48.3	0.36	1.01
	2.7	2	3.00	-0.320	48.1	0.35	1.79
0.015	3.0	3	3.31	-2.620	126.8	0.94	-1.38
	3.2	3	3.41	0.195	127.1	0.94	0.95
	3.4	3	3.61	-2.870	126.5	0.94	3.08
	5.5	4	4.39	-1.38	124.5	0.92	-2.01
	6.0	4	4.58	0.004	124.1	0.92	1.21
	6.2	4	4.65	-1.10	124.1	0.92	2.3

Table 2. Ion cycloton velocity shear instability for the PSBL parameters: $\omega_{pe}/\Omega_e=10.0$, $N_{0B}/N_{0i}=0.01$, $T_i/T_B=0.5$, $T_e/T_B=5.0$, $m_i/m_b=1.0$, $V_B/\sqrt{2}V_{tB}=10.0$, and $S=4.0$

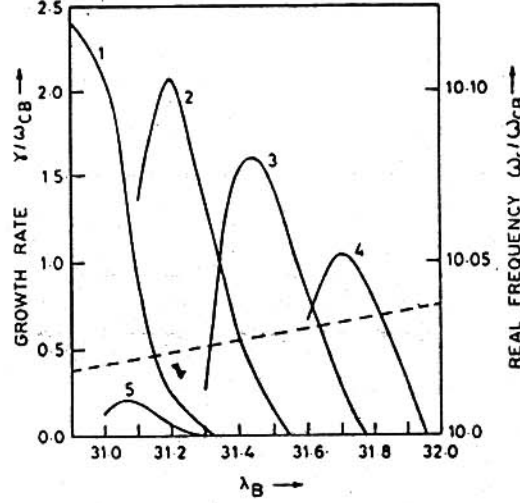| $k_\parallel/k$	λ_B	m	ω_r/Ω_B	γ/Ω_B	μ_{0i}	μ_{0e}	μ_{mB}
0.035	1.7	2	2.58	-3.77	56.3	0.42	-0.98
	1.9	2	2.71	0.29	55.9	0.41	0.38
	2.0	2	2,76	1.76	55.7	0.41	0.98
	2.1	2	2.82	0.47	55.5	0.41	1.55
	2.2	2	2.83	-0.35	55.4	0.41	2.08
0.024	3.6	3	3.61	-7.18	78.9	0.58	-0.59
	3.8	3	3.69	1.22	78.7	0.58	0.54
	4.0	3	3.78	0.30	78.5	0.58	1.58
	4.2	3	3.87	-0.94	78.5	0.58	2.55

Fig. 3 : Variation of groowth rate (solid curves) and real frequency (dashed curves) for the $m = 10$ harmonic cyclotron instability driven by velocity shear of the ion beam for PSBL parameters: $\omega_{pe}/\Omega_e=10.0$, $N_{0B}/N_{0i}=0.1$, $T_i/T_B=0.5$, $T_e/T_B=5.0$, $m_i/m_b=1.0$, $V_B/\sqrt{2}V_{tB} = 4.0$, $S=2.0$, and for $k_\parallel/k = 0.005, 0.006, 0.007, 0.008$ for the curves 1, 2, 3, and 4 respectively. Curve 5 is for $S = 1.0$ and $k_\parallel/k = 0.005$ (tken from Lakhina [28]).

Application to Plasma Sheet Boundary Layer

We expect the velocity shear parameter $S \simeq 0.05$ to 5 in the plasma sheet boundary layer. This is based on the observations which indicate intense ion flows in a thin boundary layer with thickness of 10^2 km to 10^4 km. The life time of the ion beams is typically $\sim$ (15 - 60) min [24, 43]. In view of the observations, we choose as typical parameters in the plasma sheet boundary layer the values of $N_{0B}/N_{0i} \simeq 0.1$, $V_B/\sqrt{2}V_{tB} = 4$ - 10, $S = 0.05$ - 5, $T_e/T_B = 5$, $T_i/T_B = 0.5$, ρ_B (beam Larmor radius) $= 40$ km, corresponding to $T_B \simeq 100$ eV, and $\Omega_B = 0.4$ Hz. Then from Figure 3 and Tables 1 and 2, the electrostatic noise generated by the velocity shear cyclotron instabilities would be in the frequency range 0.4 Hz $< \omega_r < 4.0$ Hz with the associated unstable transverse wavelengths $\lambda_\perp = 2\pi\rho_B/\lambda_B^{1/2}$ in the range 30 km $< \lambda_\perp < 400$ km. Since typical $k_\parallel/k \sim 0.005$ - 0.5, the noise propagates nearly transverse to the magnetic field, and is broadband in nature. The low frequency noise excited by the velocity shear instability should be observable in the plasma sheet boundary layer as the typical growth times, ~ 0.5 min or less, are generally much smaller than the characteristic life time of $\sim$ (15 - 60) min of the ion beams. Further, to have an idea of the characteristic velocity gradient scale lengths $L_v = (dV_B/V_B dx)^{-r}$ involved, the velocity shear $S =2$, for an

76

ion beam velocity of $V_B = 980$ km s^{-1}, would correspond to $L_v = 200$ km.

Interestingly, the low-frequency noise can scatter both the hot electrons and hot ions rather efficiently because of its resonant interaction with these particles. The typical electron scattering time for the $m = 1$ cyclotron instability is $\tau_s = 0.25$ (and even less for higher harmonics !). The electron scattering time is much less than the typical growth time of $\sim$ 10 min of the ion tearing mode in the plasma sheet. The ion tearing instability is stabilized by the magnetized electrons which get bunched in the region of compressed magnetic field produced by the tearing perturbations. The scattering due to the low-frequency noise could destroy these electron bunches, thus helping the ion tearing mode instability to grow [54]. It would therefore be interesting to study the effect of the low frequency noise on the tearing modes in the presence of velocity shear [55].

Application to Polar Cusp

Several groups [5, 6, 56] have observed broadband electrostatic noise (BEN) from 1.78 Hz to about 30 - 100 kHz in the polar cusp at altitudes of 2 - 10 R_E down to ionospheric heights. Various mechanisms based on ion acoustic instability or Buneman instability [57, 58], and ion cyclotron instablity [59] have been suggested to for the generation of BEN in the polar cusp.

Gurnett and Frank [6] found either keV protons flowing down (of magnetosheath origin) or proton beams (possibly accelerated ionospheric protons) streaming up the magnetic field direction at the time of BEN in the polar cusp region. Since large gradients in flow velocity of protons can occur near the cusp boundaries [60 - 61], the velocity shear instabilities discussed here may be important for exciting the low-frequency part of BEN in the polar cusp. We consider the typical polar cusp plasma parameters at the altitude range of 5 - 7 R_E as $N_{0B}/N_{0i} \simeq 0.1 - 0.3$, $\Omega_B \simeq (2.2 - 3.0$) Hz, $V_B/V_{tB} \leq 2\sqrt{2}$, $T_e \simeq 100$ eV, $T_i \sim$ a few 10 eV, $\omega_{pe}/\Omega_e \simeq (8 - 20)$, and $S \simeq 0.1 - 1$. For a 2 keV ion beam, the corresponding velocity gradient scales would be $L_v = 50 - 500$ km. We expect the cyclotron instability due to velocity shear to occur in the polar cusp for these parameters. However, the instabilty would occur in different combinations of the parameters like $k_\parallel/k$ and λ_B than those for the plasma sheet boundary layer since the beam and plasma parameters in these two regions are not the same. For example, in the polar cusp region, the $m = 2$ instabilty would occur for $\dot{V}_B/V_{tB} = \sqrt{2}$, $\lambda_B = 90$, $T_B/T_i = 50$, $T_B/T_e = 5$, $N_{0B}/N_{0i} = 0.3$, $S = 1.0$, and $k_\parallel/k = 7.2 \times 10^{-3}$ with $\omega_r = 2.145\,\Omega_B$, and $\gamma = 0.81 \times 10^{-3}\,\Omega_B$. The higher harmonics are excited for larger values of λ_B (i/e., $\lambda_B > 90$) as found for the plasma sheet boundary layer.

We must remark that Doppler shifts due to the satellite motion across the cusp field lines could mask the cyclotron structure of the modes, and the noise may appear as broadband. To estimate the Doppler shifts, $\omega' = k_\perp V_{sat}$, where V_{sat} is the satellite speed transverse to the field lines. For $\lambda_B \simeq (90 - 400)$ and $V_{sat} = 3$ km s^{-1}, we get $\omega' \simeq (3 - 5)$ Hz $> \Omega_B$. With the velocity shear of $S = 1$, we expect several harmonics (atleast upto $m = 10$ or so) to be excited simultaneously with different combinations of $k_\parallel/k$ and λ_B. This would result in the generation of the noise in the frequency range 2 Hz to about 35 Hz. This frequency range more or less matches the frequencies (e.g., 10 - 50 Hz) where the maximum intensities of the polar cusp BEN are found. Therefore, the velocity shear instability mechanism is a likely candidate for the generation of low-frequency component of polar cusp BEN.

CONCLUSION

The nonresonant modes and velocity shear modes excited by the ion beams can lead to the generation of low frequency electrostatic waves on the auroral field lines, plasma sheet boundary layer and in the cusp region. The excited LEF can have amplitudes ~ 10 mV/m to 1 V/m in the auroral acceleration region. The presence of cold electrons is an essential ingredient for Mode 1 and Mode 2 ion beam instabilty mechanism. The velocity shear cyclotron modes have characteristics similar to that of the broadband electrostatic noise (BEN), and therefore these modes may be possible candidate for the generation mechanism for the low frequency component of BEN. We must, however, emphasize that the moodes discussed here are not the only one which can be excited by the ion beams. Depending on the parameters of the magnetospheric plasma, several mechanisms may be operative at the same time.

REFERENCES

1. D. A. Gurnett, R. R. Anderson, B. T. Tsurutani, E. J. Smith, G. Paschmann, G. Haerendel, S. J. Bame, and C. T. Russell, J. Geophys. Res., 84 (1979) 7043.

2. R. R. Anderson, C. C. Harvey, M. M. Hope, B. T. Tsurutani, T. E. Eastman, and J. Etcheto, **J. Geophys. Res., 87** (1982) 2087.

3. F. Scarf, L. A. Frank, K. L. Ackerson, and R. P. Lepping, Geophys. Res. Lett., 1 (1974) 189.

4. D. A. Gurnett, L. A. Frank, and R. P. Lepping, J. Geophys. Res., 81 (1976) 6059.

5. N. D'Angelo, A. Bahsen, and H. Rosenbauer, **J. Geophys. Res.,** **79** (1974) 3129.

6. D. A. Gurnett, and L. A. Frank, **J. Geophys. Res.,** **83** (1978) 1447.

7. M. Temerin, and B. Parady, **J. Geophys. Res.,** **85** (1980) 2925.

8. M. Temerin, **J. Geophys. Res.** **83** (1978) 2609.

9. B. Hultqvist, R. Lundin, K. Stasiewicz, L. Block, P. A. Lindqvist, G. Gustafsson, H. Koskinen, A. Bahnen, T. A. Potemra, and L. J. Zanetti, ιJ. Geophys. Res., **93** (1988) 9765.

10. F. S. Mozer, C. A. Cattell, M. K. Hudson, R. L. Lysak, M. Temerin, and R. B. Torbert, *Space Sci. Rev.* **27**, 155, 1980.

11. R. L. Kaufmann, *Space Sci. Revs.* **37** (1984) 313.

12. R. R. Anderson, and D. A. Gurnett, **J. Geophys. Res.,** **78** (1973) 4756.

13. W. Bernstein, B. Hultqvist, and H. Borg, **Planet. Space Sci.,** **22** (1974) 767

14. C. T. Russell, R. E. Holzer, and E. J. Smith, **J. Geophys. Res.,** **75** (1970) 755.

15. D. A. Gurnett, **J. Geophys. Res.,** **81** (1976) 2765.

16. D. A. Gurnett, and L. A. Frank, **J. Geophys. Res.,** **82,** (1977) 1031.

17. S. Perraut, A. Roux, P. Robert, R. Gendrin, J. A. Sauvaud, J.-M. Bosqued, G. Kremser, and A. Korth, **J. Geophys. Res.,** **87** (1982) 6219.

18. H. Laakso, H. Junginger, A. Roux, R. Schmidt, and C. de Villedary, **J. Geophys. Res.,** **95** (1990) 10609.

19. J. D. Huba, N. T. Gladd, and K. Papadopoulos, **J. Geophys. Res.,** **83** (1978) 5217.

20. S. P. Gary, and T. E. Eastman, **J. Geophys. Res.,** **84** (1979) 7378.

21. F. V. Coroniti, R. W. Fredricks, and R. White, **J. Geophys. Res.,** **77** (1972) 6243.

22. G. S. Lakhina, **Planet. Space Sci.,** **24** (1976) 609.

23. K. G. Bhatia, and G. S. Lakhina, **Proc. Indian Acad. Sci. (Earth and Planet. Sci.),** **89** (1980) 99.

24. C. L. Grabbe, and T. E. Eastman, **J. Geophys Res.** **89** (1984) 3865.

25. M. Ashour-Abdalla, and H. Okuda, **Geophys. Res. lett.,** **13** (1986), 336.

26. P. B. Dusenbery, andd L. R. Lyons, **J. Geophys. Res.,** **90** (1985) 10935.

27. N. Omidi, **J. Geophys. Res.,** **90** (1985) 12330.

28. G. S. Lakhina, **J. Geophys. Res.,** **92** (1987) 12161.

29. R. Bergmann, and W. Lotko, **J. Geophys. Res.** **91** (1986) 7033.

30. R. Bergmann, I. Roth, and M. K. Hudson, **J. Geophys. Res.,** **93** (1988) 4005.

31. P. B. Dusenbery, R. E. Martin Jr., and R. M. Winglee, **J. Geophys. Res.,** **93** (1988) 5655.

32. M. Ashour-Abdalla, and D. Schriver, **Geophys. Res. lett.,** **16** (1989), 21.

33. G. S. Lakhina, **Ann. Geophysicae 11** (1993) 705.

34. T. F. Bell, and H. D. Ngo, **J. Geophys. Res.,** **93** (1988) 2599.

35. P. K. Shukla, and S. Bujarbarua, **J. Geophys. Res.,** **85** (1980) 1773.

36. M. Roy, and G. S. Lakhina, **Astrophys. Space Sci.**, **117** (1985) 111.

37. T. A. Fritz, and W. N. Spjeldvik, **J. Geophys. Res.**, **84** (1979) 2608.

38. L. M. Kistler, F. M. Ipavich, D. C. Hamilton, G. Gloeckler, B. Wilken, G. Kremser, and W. Stüdemann, *J. Geophys. Res.*, **94** (1989) 3579.

39. A. T. Y. Lui, R. W. McEntire, D. G. Sibeck, S. M. Krimigis, **J. Geophys. Res.**, **95** (1990) 20839.

40. R. Lundin, and L. Eliasson, **Ann. Geophysicae** **9** (1991) 202.

41. I. A. Daglis, E. T. Sarris, and B. Wilken, **Ann. Geophys.**, **11** (1993) 685.

42. A. G. Ghielmetti, R. G. Johnson, R. D. Sharp, and E. G. Shelley, **Geophys. Res. Lett.**, **5** (1978) 59.

43. Parks, G. K., et al., **J. Geophys. Res.**, **89** (1984) 8885.

44. L. M. Kistler, E. Möbius, B. Klecker, G. Gloeckler, F. M. Ipavich, and D. C. Hamilton, **J. Geophys. Res.**, **95** (1990) 18871.

45. W. K. Peterson, R. D. Sharp, E. G. Shelley, R. G. Johnson, and H. Balsiger, **J. Geophys. Res.**, **86** (1981) 761.

46. K. G. Bhatia, and G. S. Lakhina, **J. Plasma Phys.**, **24** (1980) 221.

47. P. Revathy, and G. S. Lakhina, **J. Plasma Phys.**, **17** (1977) 133.

48. R. Bingham, D. A. Bryant, and D. S. Hall, **Annales Geophysicae**, **6** (1988) 159.

49. N. D'Angelo, **Phys. Fluids**, **8** (1965) 1748.

50. M. Dobrowolny, **Phys. Fluids**, **15** (1972) 2263.

51. J. D. Huba, **J. Geophys. Res.**, **86** (1981) 3653.

52. A. Hasegawa, **Plasma Instabilities and Nonlinear Effects**, Springer, New York, 1975.

53. G. S. Lakhina, **Physica Scripta**, **T50** (1994) 114.

54. F. V. Coroniti, **J. Geophys. Res.**, **85** (1988) 6719.

55. G. S. Lakhina, and K. Schindler, **J. Geophys. Res.**, **93** (1988) 8591.

56. S. A. Curtis, W. R. Hoegy, L. H. Brace, N. C. Maynard, M. Suguira, and J. D. Winningham, **Geophys. Res. Lett.**, **9** (1982) 997.

57. F. L. Scarf, R. W. Fredricks, I. M. Green, and C. T. Russell, **J. Geophys. Res.**, **77** (1972) 2274.

58. R. W. Fredricks, F. L. Scarf, and C. T. Russell, **J. Geophys. Res.**, **78** (1973) 2133.

59. M. Ashour-Abdalla, and R. M. Thorne, **Geophys. Res. Lett.**, **4** (1977) 45.

60. N. D'Angelo, **J. Geophys. Res.**, **78** (1973) 1206.

61. N. D'Angelo, **Rev. Geophys.**, **15** (1977) 299.